Hindawi
Advances in Materials Science and Engineering
Volume 2021, Article ID 3573306, 9 pages
https://doi.org/10.1155/2021/3573306

Research Article

A Numerical Approach on Waste Heat Recovery through Sidewall Heat-Exchanging in an Aluminum Electrolysis Cell

Youjian Yang,[1] **Wenju Tao**,[1] **Zhaowen Wang**,[1] **and Zhongning Shi**[2]

[1]*Key Laboratory for Ecological Metallurgy of Multimetallic Mineral (Northeastern University), Ministry of Education, No. 3-11, Wenhua Road, Heping District, Shenyang 110819, China*
[2]*State Key Laboratory of Rolling and Automation, Northeastern University, No. 3-11, Wenhua Road, Heping District, Shenyang 110819, China*

Correspondence should be addressed to Youjian Yang; yangyj@smm.neu.edu.cn

Received 8 June 2021; Revised 2 July 2021; Accepted 7 August 2021; Published 26 August 2021

Academic Editor: Candido Fabrizio Pirri

This paper proposes a technical viewpoint for the recovery of waste heat in aluminum electrolysis. The idea of combining heat-generating electrolysis process and the heat-consuming alumina tube digestion process is discussed in detail. The structural design of the heat-exchanging system as well as the matching problems between the heat exchanger and cell design are also mentioned. Several major concerns including the automatic temperature regulation of the cell sidewall and the preferred selection principles for the heat medium are introduced. A 2 kA heat exchangeable cell is developed and a series of tests are carried out in the laboratory. It is found that approximate 80% of the sidewall waste heat can be recovered while the cell behaves steadily. It is also proved possible to control the thickness of the frozen ledge through adjusting the heat convection rate of the heat exchanger. The heat-exchanging system is also suitable for aluminum cells when the fluctuating wind power is applied as a major energy supply.

1. Introduction

The total primary aluminum production in China for the year 2020 has reached up to 37330 thousand metric tons, accounting for 53.7% of the world's primary aluminum production [1]. Meanwhile, the huge electricity consumption along with the primary aluminum industry covered approximately 6.8% of the China's overall electricity generation in 2020 [1]. However, the energy efficiency for the aluminum electrolysis process is about 50%, which means nearly half of the power consumption is converted and lost in the form of heat in the aluminum electrolysis cells [2]. Thus, it is very meaningful to carry out the investigation on the waste heat recovery in the aluminum reduction cells.

The heat loss in modern large-scale prebaked aluminum reduction cell can be attributed to three major paths [3–5]. (1) Heat loss from the upper parts, generally, escapes with the hot fume discharging and takes a proportion of more than 50% of the overall heat generation. This part of waste heat is difficult to recycle because the temperature of the fume is quite low for 100–180°C. (2) Heat loss from the side shells takes a proportion of nearly 30% of the overall heat generation with a surface temperature of 250–350°C, which is still not high enough for direct heat exchanging. (3) The rest heat is lost from the cell bottom and cathode busbars, which is too dispersive to recycle.

Many institutes including Hydro Aluminum [6], Pechiney Aluminum [7], and Alcoa have carried out research work on heat recycling from the side shells of the aluminum reduction cell since 1980s (refer to Figures 1 and 2). However, these technologies have not been applied widely on the commercial cells.

Siljan [6], in Hydro, proposed a method for recycling the heat emission from the side shell by installing a cooling molding SiC thermal transducer from inside of the steel shell. Lamaze et al. [7], in Pechiney, developed another method by mounting a layer of porous material on the outside surface of the cell shell, and the heat transfer medium through the porous layer was chosen as air and metallic vapor.

However, it is easy to tell the difference between these two methods. The externally installed heat exchanger is convenient for operation and maintenance and usually has a

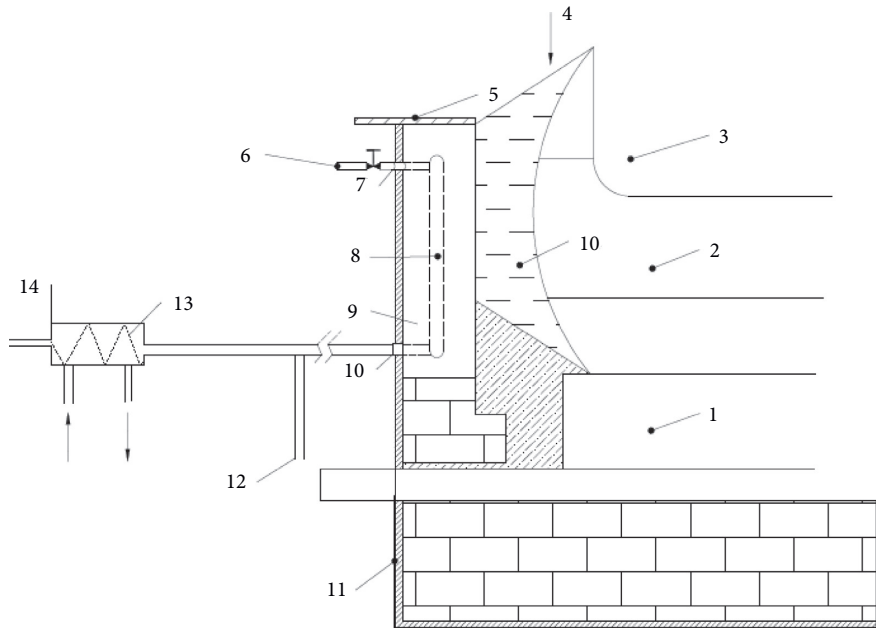

1–cathode,
2–bath,
3–anode,
4–frozen ledge,
5–steel shell,
6–air valve,
7–connector,
8–thermotube,
9–SiC material,
10–connector,
11–steel shell,
12–barometer,
13–heat conducting fin,
14–heat exchanger

Figure 1: A type of heat-exchanging aluminum reduction cell developed by Hydro Aluminum [6].

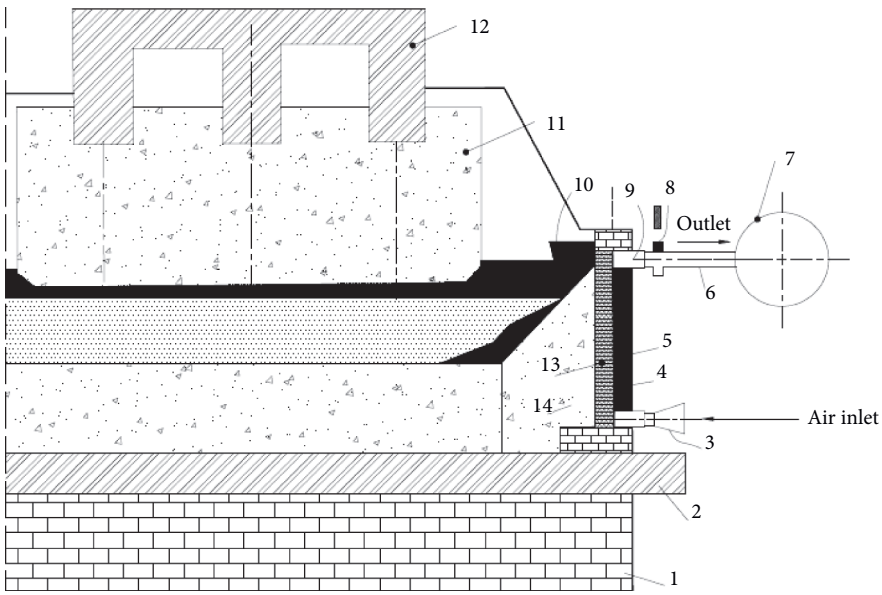

1–refractory brick,
2–cathode busbar,
3–air inlet,
4–porous material,
5–container,
6–gas outlet,
7–heat exchanger,
8–valve,
9–connector,
10–frozen ledge,
11–anode,
12–anode steel claw,
13–SiC brick,
14–paste

Figure 2: A type of heat-exchanging aluminum reduction cell developed by Pechiney Aluminum [7].

simpler structure, but it also possesses a relatively low heat transfer efficiency due to the low surface temperature of the steel-made cell shell [8]. As a contrast, the built-in exchanger enjoys higher surface temperature which could bring a higher heat transfer efficiency as well. While a high temperature and corrosive working conditions needs to be supported by a more complicated structure and restricted material selection [9]. The heat medium is usually chosen as gas (basically air) and water [6, 7]. The heat capacity of the gaseous medium is usually quite low, which means it would not be suitable for a long distance transmission; thus, the current application for the recycled heat is generally preheating cold anode and alumina.

In this paper, in order to obtain a relatively high surface temperature that promotes the heat-exchanging efficiency, a thermal insulation layer was installed inside of the side steel shells in the laboratory 2 kA aluminum reduction cell. And, the heat exchanger is mounted adjacent with the thermal insulation layer to obtain a surface temperature of more than 300°C. $NaNO_2$-KNO_3-$NaNO_3$-based molten salts was chosen as the heat medium for the transportation of the absorbed heat. The recycled heat can be directly used for the tube digestion process during primary alumina production (many aluminum plants are in proximity to alumina plants in China) or provide heat for the steam boilers.

The development of the heat recycling system for the aluminum reduction cell should be based on the existing aluminum electrolysis technology. This paper discusses a heat recovering method from inside of the side shells. It should be noted that, with the high-efficient heat-exchanging method as presented in this work, the heat balance of the reduction cell could be controlled quickly and effectively. One of the subsequent influences is that the heat-exchanging system is able to control the formation and melting of the frozen ledge by adjusting the heat flow rate through the heat exchanger. This effect is very important because the shape of the frozen ledge in the cell is very much related to the cell stability of the electrolysis process [10] and further on the current efficiency [11]. Obviously, there are several key topics that need to be considered: (1) the compatibility between the heat-exchanging system and cell structures, (2) the maintenance of the thermal balance of the cell, (3) the heat medium material and heat reapplication, and (4) equipment reliability and failure diagnosis. This work represents some innovative achievements from the previous projects supported by the National High-tech R&D Program of China (863 Program).

2. Development of the Heat-Exchanging System on Aluminum Reduction Cell

2.1. Materials and Methods

2.1.1. Structural Design of the Heat-Exchanging Aluminum Reduction Cell. Northeastern University in China started research work on high efficiency heat-exchanging aluminum reduction cell from 2002. The schematic diagram for the new-designed heat-exchanging cell is shown in Figure 3. To obtain a high surface temperature, the built-in heat exchanger was positioned close to the external surface of the SiC brick (Figure 3) [12, 13]. The nitrate molten salts was employed as the heat medium which could acquire an operation temperature as high as 650°C.

2.1.2. Selection of the $NaNO_2$-KNO_3-$NaNO_3$ System Heat-Transfer Medium. Table 1 shows a list of potential medium materials. The $NaNO_2$-KNO_3-$NaNO_3$-based molten salts can achieve a high operating temperature up to 600°C, while the synthetic heat-transfer oil (Therminol VP-1) works below 400°C. In fact, the $NaNO_2$-KNO_3-$NaNO_3$ system is usually used in the area of solar energy utilization for its large specific heat capacity and perfect thermostability under high temperature. Some pervious research achievements on the density, electric conductivity, and structure characterization have been published on academic journals and conferences [14–16].

Differential Thermal Analysis (DTA) and Thermogravimetric Analysis (TGA) testing was conducted to investigate the thermostability of the $NaNO_2$-KNO_3-$NaNO_3$-based molten salts. The DSC-TGA curves for the 30 wt%$NaNO_2$-70 wt%KNO_3 mixed salts are shown in Figure 4. The results in Figure 4 indicate that the mixed salts with this certain composition behave at an acceptable decomposition rate at 150−650°C, an operable of which is wide enough for future application.

2.1.3. Heat-Exchanging Experiments Conducted with the 2 kA Laboratory Cell. A 2 kA lab-scale aluminum reduction cell was built with the molten salts' heat-exchanging system in the Northeastern University since 2008. Several key research topics were launched with this system intermittently in the following years. Figure 5 shows photos of this heat-exchanging system.

With this self-designed system, the correlations between several operational parameters, including the total power input, medium flow rate, temperature variation of the medium, surface temperature of the heat exchanger, heat transfer efficiency, and heat exchange capability were investigated. Established on these fundamental research studies, the design principles for large-scale heat-exchanging cell and auxiliary thermal cycling system are proposed.

2.1.4. Establishment of the Simulation Models. The commercial software ANSYS is employed for the computer simulation of a 2 kA laboratory-designed heat-exchanging cell. A mathematical model of the temperature field was built to investigate the effects of heat flux fluctuation on the electrolysis process.

(1) Governing Equations. The governing equations for the heat transfer and electrical potential distribution are [17]

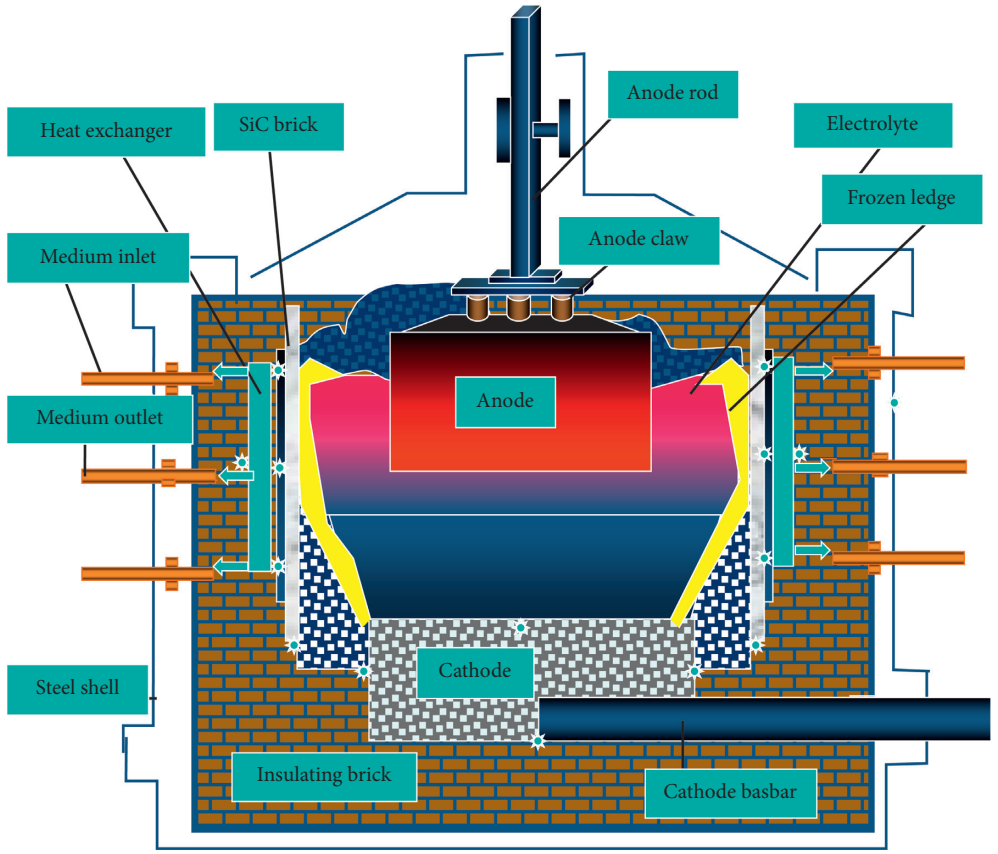

Figure 3: The schematic diagram of the heat-exchanging aluminum reduction cell developed by the Northeastern University of China [12, 13].

Table 1: Comparison of several selected heat-transfer mediums [14–16].

Properties		Solar salt	Hitec	Hitec XL	$LiNO_3$	Therminol VP-1
Compositions	KNO_3	60	53	7	—	—
	$NaNO_2$	—	40	—	—	—
	$NaNO_3$	40	7	45	—	—
	$Ca(NO_3)_2$	—	—	48	—	—
Melting point (°C)		220	142	120	120	13
Maximum service temperature (°C)		600	535	500	550	400
Properties when operating at 300°C or below	Density ($kg{\cdot}m^{-3}$)	1899	1640	1992	—	815
	Viscosity (mPa·s)	3.26	3.16	6.37	—	0.20
	Specific heat capacity ($J{\cdot}kg^{-1}{\cdot}K^{-1}$)	1495	1560	1447	—	2319

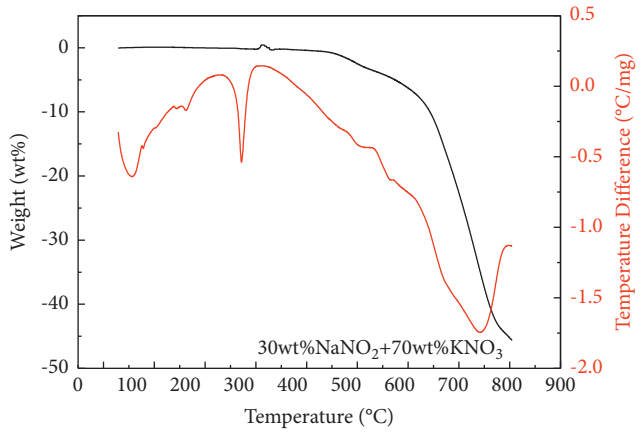

Figure 4: The DSC-TGA curves for the 30 wt%$NaNO_2$-70 wt%KNO_3 mixed salts.

Figure 5: Photos of the 2 kA lab-scale heat-exchanging aluminum reduction cell.

$$\frac{\partial}{\partial x}\left(\lambda_x \frac{\partial T}{\partial x}\right) + \frac{\partial}{\partial y}\left(\lambda_y \frac{\partial T}{\partial y}\right) + \frac{\partial}{\partial z}\left(\lambda_z \frac{\partial T}{\partial z}\right) + q(x, y, z) = 0,$$

$$\nabla[\sigma \nabla V] = 0, \tag{1}$$

where T is temperature, k is the thermal conductivity, r is the electrical conductivity, V is the electrical potential, and q is the heat generation rate per unit volume (Joule effect). For a small volume, when the current flows, the Joule heat per unit volume is given by the following equation:

$$q = \sigma \times (-\nabla V)^{-2}. \tag{2}$$

(2) Thermoelectric Coupled Model. A three-dimensional (3D) model is necessary to analyze the thermoelectric field. Because of the symmetry of the cell, only half of the geometric model was built as a computational domain (Figure 4). The commercial software ANSYS (Ansys Inc., Canonsburg, PA) was used for the coupled thermoelectric calculation. The thermoelectric coupled element SOLID69 was used to transmit heat and current as well as generate Joule heat. The thermal-only element SOLID70 was used to simulate the heat transfer for thermal insulating materials. CONTACT170 and TARGET173 were used to simulate the thermal contact.

(3) Boundary Conditions.

Electrical. The end of the collector bar was at zero potential. On the top surface of the anode rod, constant current was entered at a constant floating potential. This was achieved by coupling the voltage on the surface nodes, whereas constant forcing current was applied on one of its node [18].

Thermal. The temperature of the electrolyte and metal pad was assumed to be uniform. Heat losses from the shell surface to ambient air occurred by convection. Moreover, the convective heat-transfer coefficient between the melt and ledge was defined as the thermal contact conductance coefficient [19, 20].

2.2. Results and Analysis

2.2.1. Optimization of the Temperature Fields for the Heat-Exchanging Cell. Figure 6 shows the simulated temperature distribution of the 2 kA laboratory cell. The high-temperature zone of the cell concentrated at the anode and inter-electrode regions, which made the electrolysis process essentially be a quite stable course.

Figure 7 shows the simulated heat-flux vectors in the 2 kA cell. It demonstrates that a large proportion of the heat generation was lost or transferred from the top and sides of the cell, and the cathode busbar took away a certain portion of heat as well.

For a typical industrial aluminum electrolytic cell, the distribution of lost heat is approximately: 50% from the top, 30%–40% from the sides, and 10%–20% from the bottom [21–24], and the similar results were also obtained with the 2 kA heat-exchanging cell by shutting off the heat medium. As a contrast, for the heat-exchanging cells in this study, the heat exchanger took away nearly 46% of the released heat from the cell, about 32% of heat escaped from the top, 17% escaped from the side, and 5% dismissed from the bottom.

2.2.2. Validation of the Numerical Models. Table 2 shows a comparison between the simulated temperature results and the corresponding measured values. It is found that these results show good agreement with each other, indicating a reliable calculation process.

As a result of the heat exchanger installed on the cell side wall, the temperatures of the cell side shell ($58 \pm 2^{\circ}$C), cathode busbar ($108 \pm 2^{\circ}$C), and cell bottom surface ($67 \pm 2^{\circ}$C) are lower than that of the typical industrial cell. It suggests that the heat exchanger has significant effect on the heat balance of the cell; meanwhile, the employment of this technology on the industrial cell requires systematic study and redesign of the cell heat balance.

The recycled heat with a temperature of 370–380°C could be used directly on the tube digestion process for primary alumina production. And, it is also technically feasible to use the waste heat for power generation when the heat-exchanging system works above 400°C. Through this system, a large amount of energy saved in aluminum plants can be reused in alumina plants, which guarantees a realistic prospect for this technology.

2.2.3. Aluminum Electrolysis Process under Variable Current. Potline current fluctuation during the electrolysis process tests the adjusting ability on the thermal balance of the reduction cell [25–27]. A sudden change on the potline

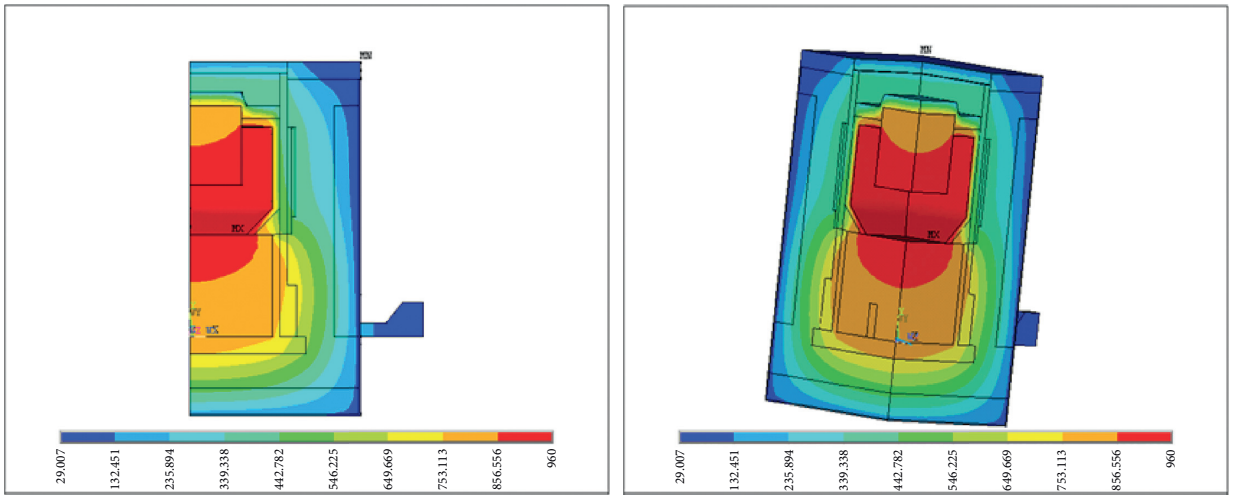

Figure 6: ANSYS simulation results of the temperature gradients in the 2 kA laboratory heat-exchanging cell.

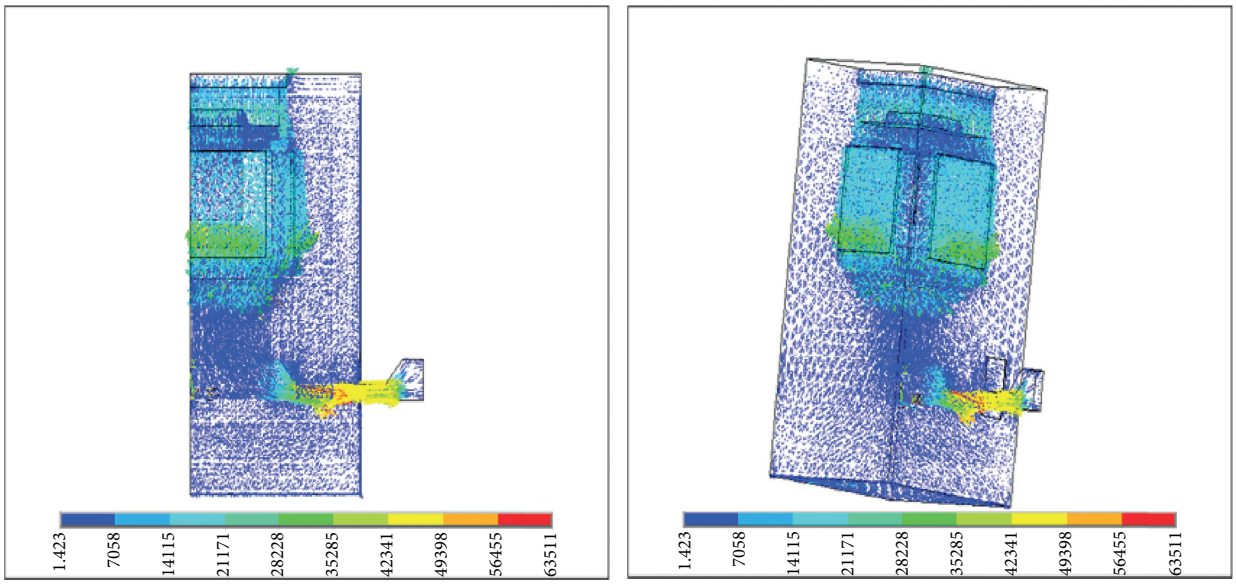

Figure 7: ANSYS simulation results of the heat-flux vectors in the 2 kA laboratory heat-exchanging cell.

Table 2: Comparison of the measured temperature values and ANSYS simulation results.

Position	ANSYS simulated temperature (°C)	Measured temperature on the 2 kA cell (°C)
Average temperature of the heat exchanger	385	379 ± 2
Side shell		
Top	46–51	46 ± 2
Middle	56–64	58 ± 2
Bottom	42–46	45 ± 2
Cathode busbar	101–124	108 ± 2
Bottom of the cell	71	67 ± 2
Lower surface of the cathode block	811	817 ± 2

current directly influences the energy supply for the whole process and usually causes a rapid temperature fluctuation in the electrolyte, which essentially refers to a shift of the previously established thermal balance.

The energy balance for the aluminum reduction cell can be expressed as

$$W_P = W_E + W_H, \tag{3}$$

where W_P refers to the total power supply for the reduction cell, determined by cell resistance R and potline current I, W_E refers to the energy consumption in the electrolysis reaction, and W_H refers to the energy lost in the form of heat.

The heat loss of the cell can be derived from

$$W_H = A \cdot K \cdot (T - T'), \tag{4}$$

where A is the equivalent heat conducting area, K is the total heat conductivity coefficient, T and T_E are the temperatures of the electrolyte and heat exchanger at I, respectively, and T' and T_E' are the temperatures of the electrolyte and heat exchanger at $(I + \Delta I)$, respectively.

When the current varies from I to $(I + \Delta I)$, the change in the total power supply is

$$\Delta W_P = (I + \Delta I)^2 \cdot R - I^2 \cdot R = 2I \cdot \Delta I \cdot R + \Delta I^2 \cdot R. \tag{5}$$

Correspondingly, the variation in heat loss is

$$\Delta W_H = A \cdot K \cdot (T' - T_E') - A \cdot K \cdot (T - T_E). \tag{6}$$

So, the net energy change of the cell can be expressed as

$$\Delta W_P - \Delta W_H = 2I \cdot \Delta I \cdot R + \Delta I^2 \cdot R - [A \cdot K \cdot (T' - T_E')] - [A \cdot K \cdot (T - T_E)]. \tag{7}$$

This energy, $(\Delta W_P - \Delta W_H)$, is stored in the cell, causing temperature changes of the electrolyte and metal pad. Assuming that a new thermal balance state is established after a time period of τ, the temperature change of the melts can be deduced as

$$T' - T = \left[\frac{\left(2I \cdot \Delta I \cdot R + \Delta I^2 \cdot R\right)}{\left(C_{p1m1} + C_{p2m2} + A \cdot K \cdot \tau\right)}\right] \cdot \tau, \tag{8}$$

where C_{p1} and C_{p2} are the specific heat capacity of liquid aluminum and molten electrolyte, respectively, and m_1 and m_2 are the mass of the aluminum and electrolyte in the cell, respectively.

Equation (6) can also be transformed to

$$\frac{C_p m}{\tau} + A \cdot K = \frac{\left(2I \cdot \Delta I \cdot R + \Delta I^2 \cdot R\right)}{\Delta T}, \tag{9}$$

where $C_p m = C_{p1} m_1 + C_{p2} m_2$, $\Delta T = T' - T$.

In equation (9), the component $(2I \cdot \Delta I \cdot R + \Delta I^2 \cdot R)/\Delta T$, W/°C, indicates the required extrapower supply for one unit change of the melts temperature. The component $C_p m/\tau$, W/°C, indicates the energy increase of the melts for one unit increase in temperature. The component $A \cdot K$, W/°C, indicates the extrathermal power of the cell for one unit change of the melts temperature, describing the heat releasing/adjusting ability of the cell.

It can be derived that the influences of the current fluctuation on the melts' temperature depend on three major aspects:

(1) The extrathermal power of the cell (component $A \cdot K$ in equation (9), or named as "extrathermal power of the cell" in this paper, indicating the ability of heat releasing or adjusting for the specific cell)

(2) The $(A \cdot K)$ value in equation (9) is a variable that is strongly related to the cell structure design; with a heat-exchanging system, the $(A \cdot K)$ value can easily be adjusted to match the variation of potline current

(3) The heat absorption rate of the melts (component $C_p m/\tau$ in equation (9))

Since the degree of tolerance for the potline current variation essentially lies within the reasonable temperature range of the electrolyte [27, 28], the amplitude of the current variation is able to be calculated through the data obtained from experimental measured data and numerical simulation.

The ANSYS model, as previously described, was used to obtain the thermoelectric fields under different cell operating conditions for both nonheat-exchanging condition (traditional cell) and heat-exchanging condition. The electrolyte temperatures were chosen as 955°C, 960°C, 965°C, 970°C, and 975°C, respectively. Potline currents were extended to 270 kA, 300 kA, 315 kA, and 330 kA, respectively, to investigate the effect of cell operation temperature and potline current on the heat-exchanging ability.

The heat-releasing/-adjusting ability (described as component $A \cdot K$ in equation (9)) of the heat-exchanging cell and traditional cell are then compared in Figures 8 and 9, respectively, with the change of cell operating temperature and potline current.

The relationships between $(A \cdot K)$ value and electrolyte temperature for the traditional cell and heat-exchanging cell are shown in Figure 8, respectively.

From Figure 8, it is obvious that the heat-releasing/-adjusting ability (described as $A \cdot K$) of the heat-exchanging cell is significantly higher than that of the traditional cell without heat-exchanging technology at 955–975°C. The $(A \cdot K)$ value increases with the increase of electrolyte temperature, which indicates that the affordability to current fluctuation of the cell gets better at higher operating temperature.

Figure 9 shows the relationships between the $(A \cdot K)$ value and potline current for the traditional cell and heat-exchanging cell, respectively.

From Figure 9, it is found that the $(A \cdot K)$ value increases linearly with increasing potline current under the same electrolyte temperature. And, it is also apparent that the heat-releasing/-adjusting ability (described as $A \cdot K$) of the heat-exchanging cell is significantly higher than that of the traditional cell.

Based on the results shown in Figures 8 and 9, the $C_p m/\tau$ value in (7) approximates to constant when the temperature change (ΔT) is regarded as zero in a very short period, while the sudden rise in potline current can be compensated by quickly adjusting to the heat-exchanging system.

Further calculation proved that the tolerance against current fluctuation for the traditional 300 kA commercial

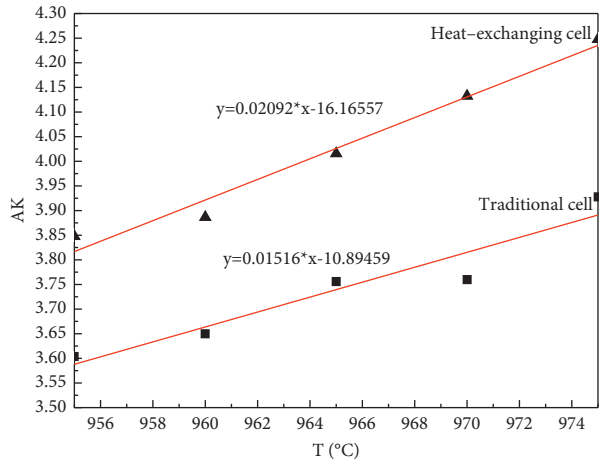

Figure 8: The relationships between (A·K) value and electrolyte temperature for the traditional cell and heat-exchanging cell, respectively (300 kA).

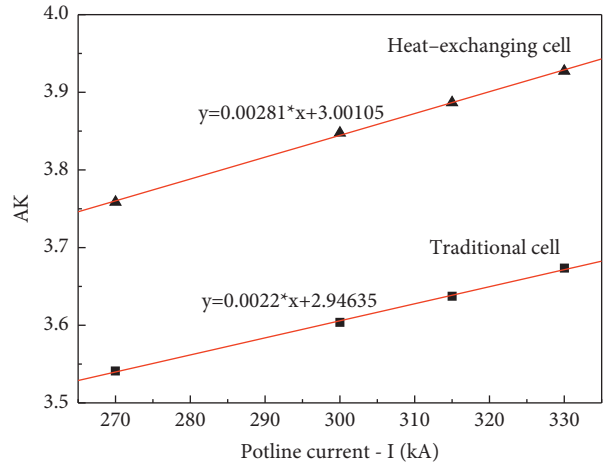

Figure 9: The relationships between the (A·K) value and potline current for the traditional cell and heat-exchanging cell, respectively (960°C).

cell is approximately 0–10%, to ensure the electrolyte temperature fluctuation less than 10°C. However, this value is significantly promoted to 20%–40% for the heat-exchanging cell proposed in the present paper.

2.2.4. Economy and Social Benefit Expectation. The employment of heat-exchanging technology on aluminum electrolytic cell has several benefits [29, 30]. For the operation of the heat-exchanging cells, the local heat balance could be managed correspondingly, and the electrolysis process could remain stable regardless the heat variation due to the changes in potline current [31–33]. For the same mechanism, the local cell condition could be managed and improved to obtain a higher current efficiency.

According to the research work carried out in the present paper, cell with this kind of heat-exchanging technology could undertake current fluctuation of 40% in maximum, which enables the introduction of clean energy such as unstable wind and solar power into the energy system for industrial aluminum electrolysis. It is estimated that the wind power utilization coefficient of the matched wind farm can be increased from 0.177 to 0.27. Meanwhile, the average price of the power for the aluminum smelter can be reduced due to the usage of the nongrid wind power.

At the same time, the aluminum plant works as the adjustable load (since the potline current of the cell can be adjusted) at the demand side of the power grid. In this way, the fluctuation from the unstable wind and solar power could be greatly reduced; subsequently, the ratio of the unstable energy is able to be increased to some extent.

Besides, the recycled heat with a temperature of 370–380°C could be used directly on the tube digestion process for primary alumina production, and it is also technically feasible to use the waste heat for power generation when the heat-exchanging system works above 400°C.

3. Conclusions

Years of investigation confirmed that it is feasible to employ a molten salt heat-exchanging system for the waste heat recovery in the aluminum electrolysis cell. This work provides fundamental basis for the future tests on industrial cells. Five major conclusions are derived from this work:

(1) Heat transfer medium based on the $NaNO_2$-KNO_3-$NaNO_3$ system is suitable for recycling high-temperature waste heat, which can be used to the tube digestion process during primary alumina production.

(2) The molten salt circulating system was designed as well as the built-in heat exchanger on the 300 kA commercial aluminum reduction cell.

(3) The composition of the heat transfer medium was proposed based on systematic research studies on the physiochemical properties of $NaNO_2$-KNO_3-$NaNO_3$ system molten salts.

(4) Laboratory tests were carried out on a self-designed 2 kA heat-exchanging cell. The results displayed that nearly 80% (maximum) of the waste heat from the side shell could be recovered in terms of steady operation. Referring to the prospects of this technology, the artificial control on the frozen ledge could be realized by adjusting operational parameters of the heat-exchanging system.

(5) The heat-exchanging aluminum reduction cell is essentially suitable for unstable energy source such as wind power, copping with differential power prices policy, or consuming excessive power from nuclear power station instead of prevailing reservoir hydropower plant.

Data Availability

The data used to support the findings of this study are included within the article. More supported data can be obtained from the corresponding author upon request or from

the Northeastern University's library: graduation thesis part and the work of Prof. Zhaowen Wang's research group.

Conflicts of Interest

The authors declare that there are no conflicts of interest regarding the publication of this paper.

Acknowledgments

The authors would like to acknowledge financial supports from the National Natural Science Foundation of China and the Fundamental Research Funds for the Central Universities (Grant nos. N2025033, 51804069, and 51974081).

References

[1] "Aluminum Corporation of China Limited, Annual report of aluminum corporation of china LTD," *Aluminum Corporation of China Limited*, Beijing, China, 2020.

[2] Y. Ladam, A. Solheim, M. Segatz, and O.-A. Lorentsen, "Heat recovery from aluminium reduction cells," *Light Metals 2011*, pp. 393–398, 2011.

[3] K. Eika and R. Skjeggstad, *Light Metals*, p. 277, 1993.

[4] M. Wan, Y. Wang, and J. Liu, "Heat dissipating capacity of aluminum reduction cell and its distribution rule," *Light Metals*, vol. 6, p. 31, 2006.

[5] J. Wang, Y. Zhang, and H. Chen, "Views on the heat lossing distributing of large-scale aluminum smelting cells in China," *Light Metals*, vol. 12, p. 22, 2007.

[6] O. J. Siljan, "Non Ferrous Metals and Minerals," The Ninth Internation of congress, Karsnoyark, Russia, U. S. Patent 0237305A1), 2006.

[7] A. P. Lamaze, R. Laucournet, and C. Barthelemy, "Electrolytic cell with a heat exchanger," Patent Application Publication, Alexandria, Egypt, U. S. Patent (0271996A1), 2008.

[8] G. Pia, J. Cai, Z. Zhang, and S. Liu, "Advances in modelling of heat and mass transfer in porous materials," *Advances in Materials Sciences and Engineering*, vol. 7089718, p. 1, 2019.

[9] J. Li, X. Han, P. Zhou, X. Sun, and N. Chang, "Comprehensive analysis of fault diagnosis methods for aluminum electrolytic control system," *Advances in Materials Sciences and Engineering*, vol. 975317, p. 1, 2014.

[10] S. Zeng, S. Wang, and Y. Qu, "Control of temperature and aluminum fluoride concentration based on model prediction in aluminum electrolysis," *Advances in Materials Sciences and Engineering*, p. 1, 2014.

[11] N. A. A. Majid, M. P. Taylor, J. J. J. Chen, and B. R. Young, "Aluminium process fault detection and diagnosis," *Annals of Materials Science & Engineering*, vol. 682786, pp. 1–11, 2015.

[12] C. Ma, X. Qi, and D. Wang, "A waste heat recycling system and apparatus for aluminum reduction cell," *Energy Saving Nonferr. Metall*, vol. 4, p. 67, 2009.

[13] Z. Wang, B. Gao, and Z. Shi, "A fundermental study on waste heat recycling from aluminum reduction cells," *Journal of Materials and Metallurgy*, vol. 9, p. 8, 2010.

[14] B. Gao, F. Liu, and Z. Wang, *Journal of North University of China (Natural Science Edition)*, vol. 31, p. 696, 2010.

[15] F. Liu, B. Gao, S. Wang, Z. Shi, and Z. Wang, "Measurement and estimation for density of NaNO2-KNO3-NaNO3 ternary molten salts," in *Proceedings of the World Non-Grid-Connected Wind Power and Energy Conference*, Nanjing, China, November 2009.

[16] B. Gao, F. Liu, Z. Wang, and W. Gao, *The 10th China-Russia System on Advanced Materials and Technologies*, Center of European Reform, London, UK, 2009.

[17] M. Blais, M. Désilets, and M. Lacroix, "Optimization of the cathode block shape of an aluminum electrolysis cell," *Applied Thermal Engineering*, vol. 58, no. 1-2, pp. 439–446, 2013.

[18] D. Richard, M. Fafard, R. Lacroix, P. Cléry, and Y. Maltais, "Aluminum reduction cell anode stub hole design using weakly coupled thermo-electro-mechanical finite element models," *Finite Elements in Analysis and Design*, vol. 37, no. 4, pp. 287–304, 2001.

[19] W. Tao, L. Wang, Z. Wang et al., "Impact of the usage of a slotted collector bar on thermoelectric field in a 300-kA aluminum reduction cell," *Journal of Occupational Medicine*, vol. 67, no. 2, pp. 322–329, 2015.

[20] W. Tao, T. Li, Z. Wang et al., "Impact of the usage of a slotted cathode carbon block on thermoelectric field in an aluminum reduction cell," *Journal of Occupational Medicine*, vol. 67, no. 5, pp. 929–937, 2015.

[21] J. Grandfield, "Update on the aluminum industry response to climate change," *Light Metal Age*, vol. 2, p. 40, 2020.

[22] N. Depree, R. Düssel, P. Patel, and T. Reek, "The 'virtual battery' - operating an aluminium smelter with flexible energy input," *Light Metals 2016*, pp. 571–576, 2016.

[23] M. Taylor and J. Chen, *The Chemical Engineer-IChemE*, vol. 891, p. 52, 2015.

[24] M. P. Taylor, R. Etzion, P. Lavoie, and J. Tang, "Energy balance regulation and flexible production: a new frontier for aluminum smelting," *Metallurgical and Materials Transactions A*, vol. 1, no. 4, pp. 292–302, 2014.

[25] P. Lavoie, M. P. Taylor, and J. B. Metson, "A review of alumina feeding and dissolution factors in aluminum reduction cells," *Metallurgical and Materials Transactions B*, vol. 47, no. 4, pp. 2690–2696, 2016.

[26] J. Liu, M. Taylor, and M. Dorreen, "Response of cryolite-based bath to a shift in heat input/output balance," *Metallurgical and Materials Transactions B*, vol. 48, no. 2, pp. 1079–1091, 2017.

[27] J. Liu, M. Taylor, and M. Dorreen, "Responses of lithium-modified bath to a shift in heat input/output balance and observation of freeze-lining formation during the heat balance shift," *Metallurgical and Materials Transactions B*, vol. 49, no. 1, pp. 238–251, 2018.

[28] M. M. R. Dorreen, R. G. Haverkamp, A. Jassim et al., "Influence of heat transfer on anode reactions when electrowinning metal from its oxides dissolved in molten fluorides," *Journal of the Electrochemical Society*, vol. 164, no. 8, pp. H5108–H5118, 2017.

[29] L. Vogel, C. Schenuit, and L. Jian, *Industrial Demand Side Flexibility in China, Deutsche Energie-Agentur GmbH (Dena)*, German Energy Agency, 2019.

[30] D. Wong, B. Welch, P. Nunez, L. Dion, and A. Spirin in *Proceedings of the 37th International ICSOBA Conference*, p. 735, Krasnoyarsk, Russia, September 2019.

[31] M. Taylor and B. Welch, "Bath/freeze heat transfer coefficients: experimental determination and industrial application," *Light Metals*, p. 781, 1985.

[32] J. Chen, C. Wei, S. Thomson, B. Welch, and M. Taylor, "Study of cell ledge heat transfer using an analogue ICE-water model," *Light Metals*, p. 285, 1994.

[33] M. Dupuis and W. Haupin, "Performing fast trend analysis on cell key design parameters," *Light Metals*, p. 255, 2003.